Supporting Information

Thermoelectric Properties of Sub-stoichiometric Electron Beam Patterned Bismuth Sulfide

Jose Recatala-Gomez,[1,2] Hong Kuan Ng,[1,3] Pawan Kumar,[1] Ady Suwardi,[1] Minrui Zheng,[4] Mohamed Asbahi,[1] Sudhiranjan Tripathy,[1] Iris Nandhakumar,[2*] Mohammad S. M. Saifullah[1*] and Kedar Hippalgaonkar[1,5*]

[1] Institute of Materials Research and Engineering, Agency for Science, Technology and Research (A*STAR), 2 Fusionopolis Way, Singapore 138634, Republic of Singapore

[2] Department of Chemistry, University of Southampton, University Road, Highfield, Southampton SO17 1BJ, United Kingdom

[3] Department of Physics, Faculty of Science, 2 Science Drive 3, National University of Singapore, Singapore 117551, Republic of Singapore

[4] Department of Electrical and Computer Engineering, National University of Singapore, 21 Lower Kent Ridge Road, Singapore 117576, Republic of Singapore

[5] School of Material Science and Engineering, Block N4.1, 50 Nanyang Avenue, Nanyang Technological University, Singapore 639798, Republic of Singapore

Corresponding Authors

*E-mail: kedar@ntu.edu.sg, saifullahm@imre.a-star.edu.sg , iris@soton.ac.uk

Supporting Information S1: Detailed XPS analysis

This section further elaborates on the XPS data, obtained for sub-stoichiometric Bi_2S_3 annealed in vacuum at different temperatures. The XPS survey spectra shown in Figure S1(a) (up to 1100 eV) showed the presence of four elements: bismuth, sulfur, carbon and oxygen. The elements were recorded for the corresponding regions of Bi 4f, S 2s, C 1s, and O 1s. All spectra were calibrated with respect to adventitious carbon, C 1s peak at 285 eV, with an associated uncertainty of 0.2 eV.[1]

Figure 3(b) shows the core-levels of the Bi 4f spectrum with the well-separated spin-orbit components (splitting parameter equal to 5.3 eV) corresponding to the doublet $4f_{7/2}$ and $4f_{5/2}$, with peak positions at 158.51 eV and 163.83 eV, respectively.[2] The doublet at 159.10 eV and 164.41 eV corresponds to Bi $4f_{7/2}$ and Bi $4f5_{/2}$ in Bi_2O_3, which is in good agreement with the results of Morgan *et al.*[3] The two peaks centred at 161.01 eV and 162.29 eV correspond to the spin orbit components of the core-levels of S 2p, namely, S $2p_{3/2}$ and S $2p_{1/2}$. The separation between them is equal to 1.28 eV, which is slightly off from the ideal value of 1.16 eV, but the binding energies are still in good agreement with the reference values reported by Grigas *et al.* for single crystal bismuth sulfide.[4]

Figure S1 shows the core-level of S 2s, which deconvolutes into two peaks, centred at binding energies of 225.60 eV and 232.52 eV. These can be assigned to S 2s bound to Bi and SO_x species (most likely formed as a result of the sulfur removal during vacuum annealing), respectively.[5]

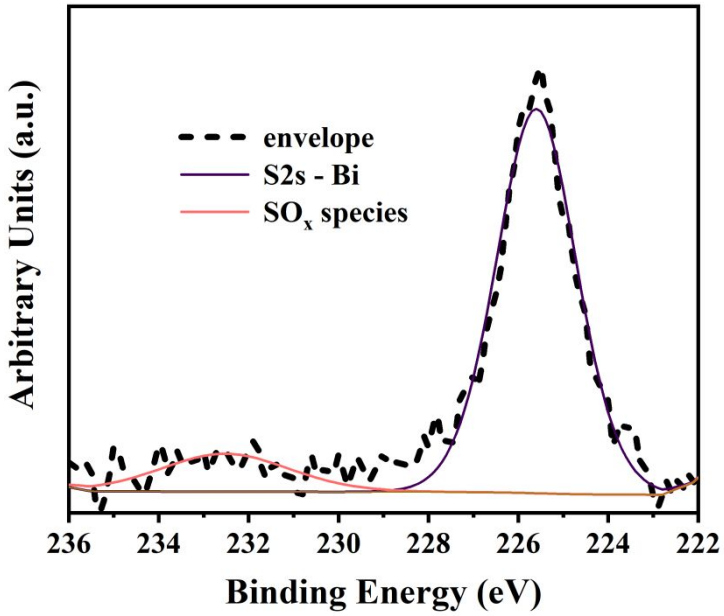

Figure S1. XPS core level spectra of S 2s acquired from the film annealed at 350 °C.

Supporting Figures

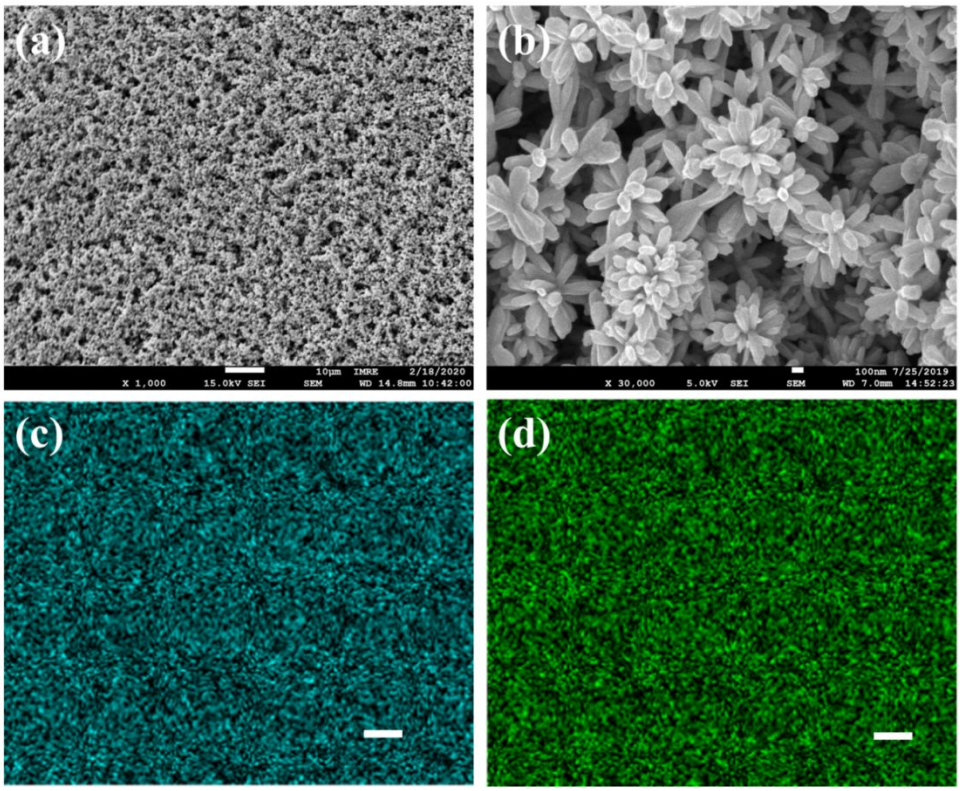

Figure S2. Material characterization of pristine bismuth sulphide (Bi_2S_3): (a) Top view SEM image of the sample, (b) flower-like features comprising the film and EDX map of (c) bismuth, (d) sulfur (inset bars are 10 μm). The elemental composition of this film was determined to be 40.90 at. % of Bi and 59.10 at. % of sulfur. Both elements are equally distributed with no clusters observed.

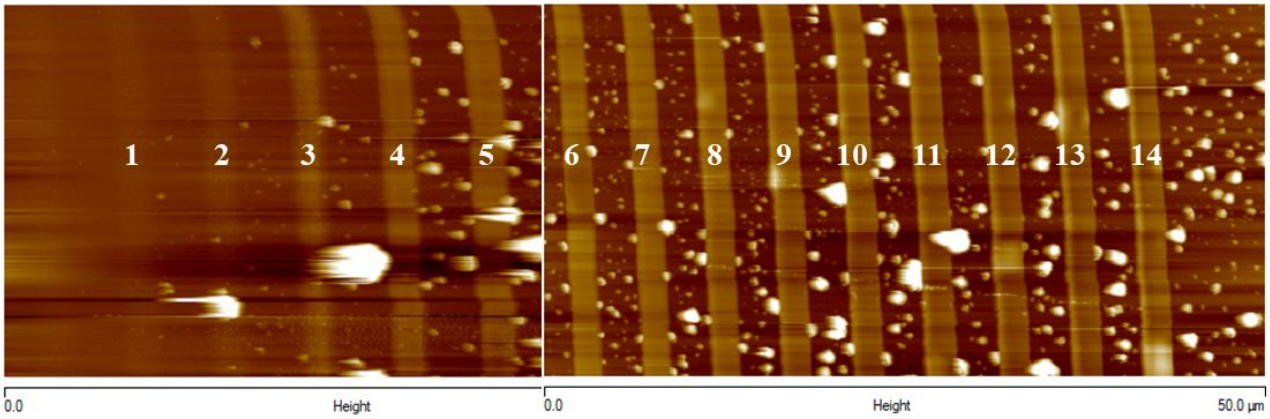

Figure S3. AFM topography images of pre-defined lines exposed at different doses. With dose and height, Figure 2(b) was plotted.

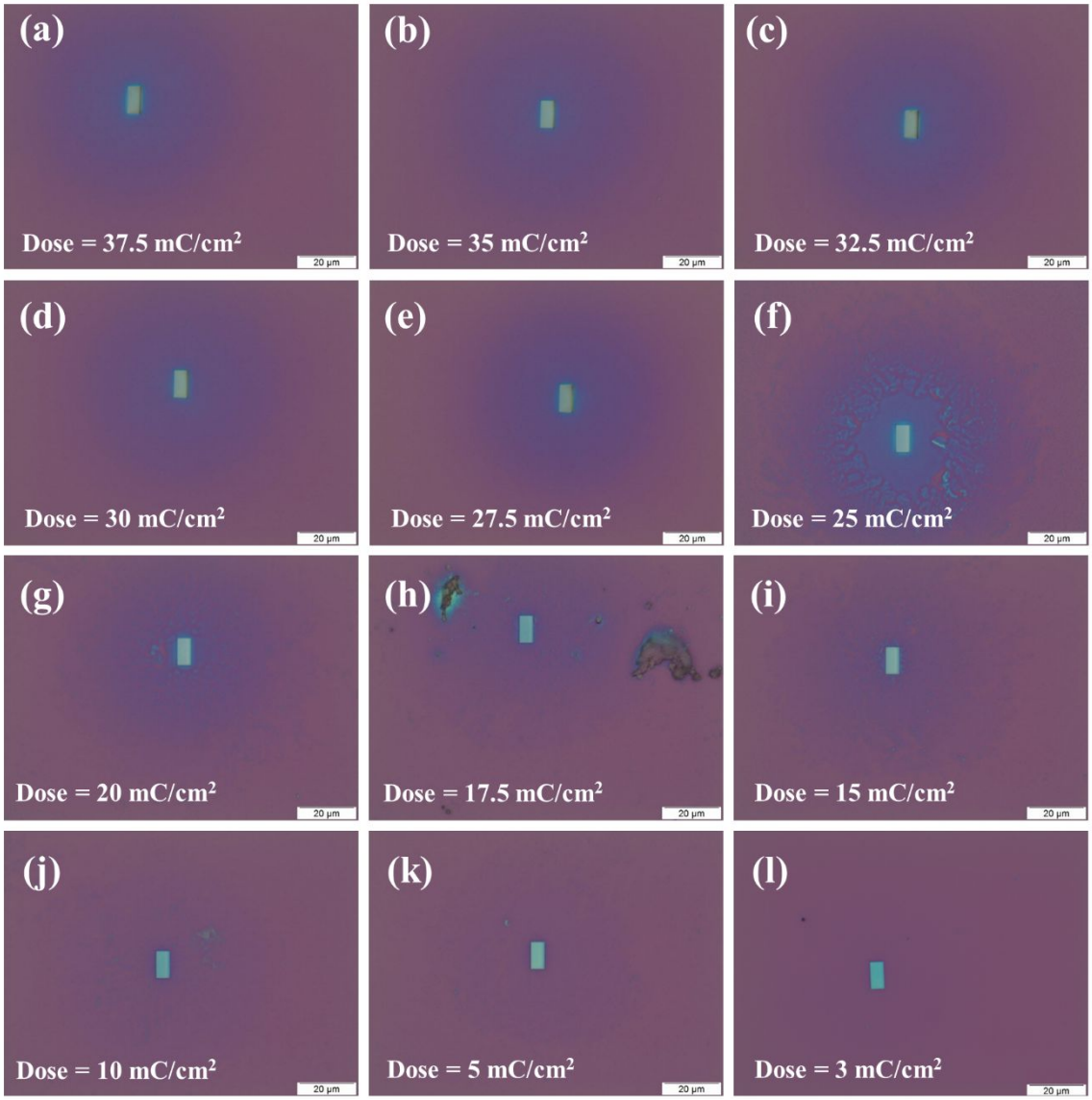

Figure S4. Optical images of bismuth(III) ethylxanthate resist films exposed at different doses. A dose equal to 3 mC/cm^2 was chosen for the patterning of the films because it does not show overexposure.

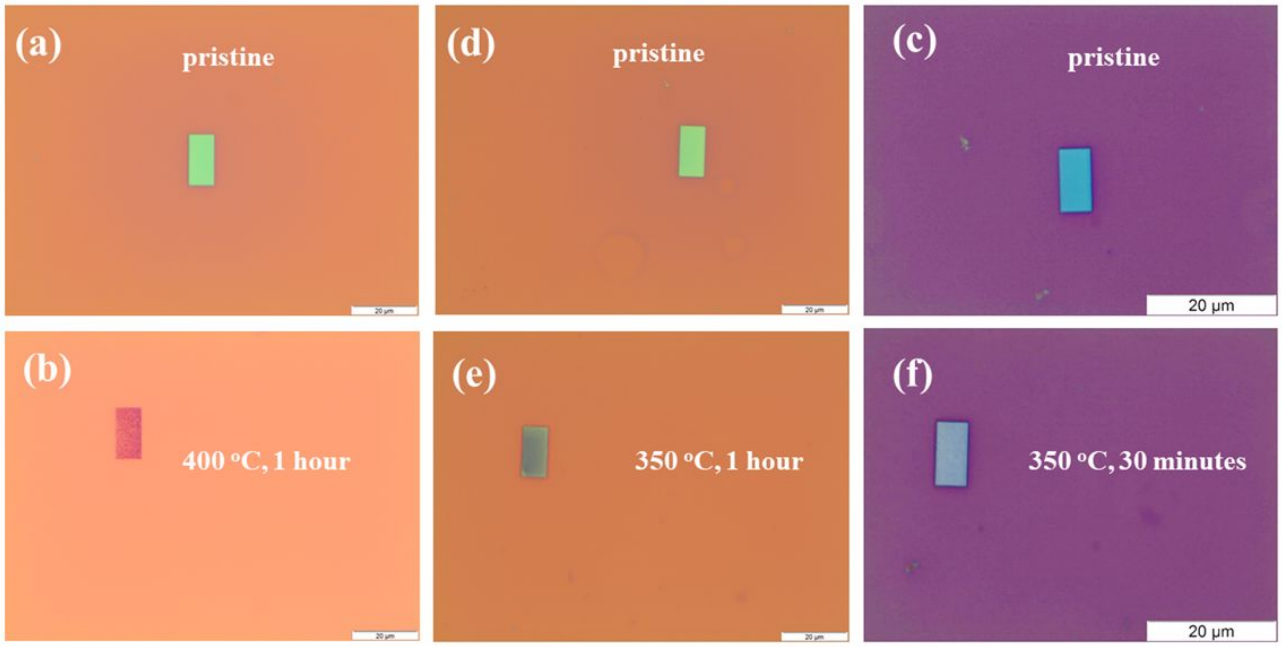

Figure S5. Optical images of patterned bismuth(III) ethylxanthate resist films annealed at different temperature and time. Heat-treatment temperature of 400 °C resulted in delamination of the film from the substrate, thus being the upper boundary of annealing temperature. A temperature of 350 °C for 30 minutes was chosen as heat treatment condition for the removal of organic matter from the patterned film, as it gives the best compromise between crystalline quality and mechanical stability.

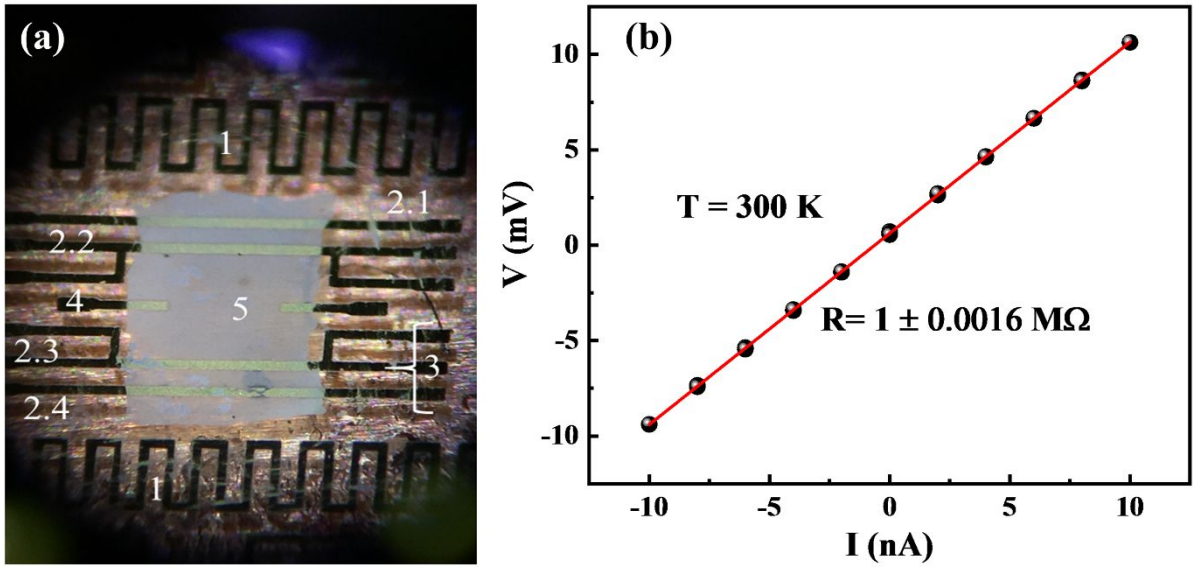

Figure S6. (a) Device for thermoelectric measurements. The elements are: (1) heaters, (2) 4 resistivity lines for 4 probe measurements (2.1: I^+, 2.2: V^+, 2.3: V^-, 2.4: I^-), (3) thermometers, (4) Hall bars for Hall measurements and (5) pristine Bi_2S_3 thin film ready to be measured. (b) Room temperature four probe resistivity measurement of pristine Bi_2S_3. The slope of the linear fit corresponds to the resistance of the sample, R = 1 ± 0.0016 MΩ.

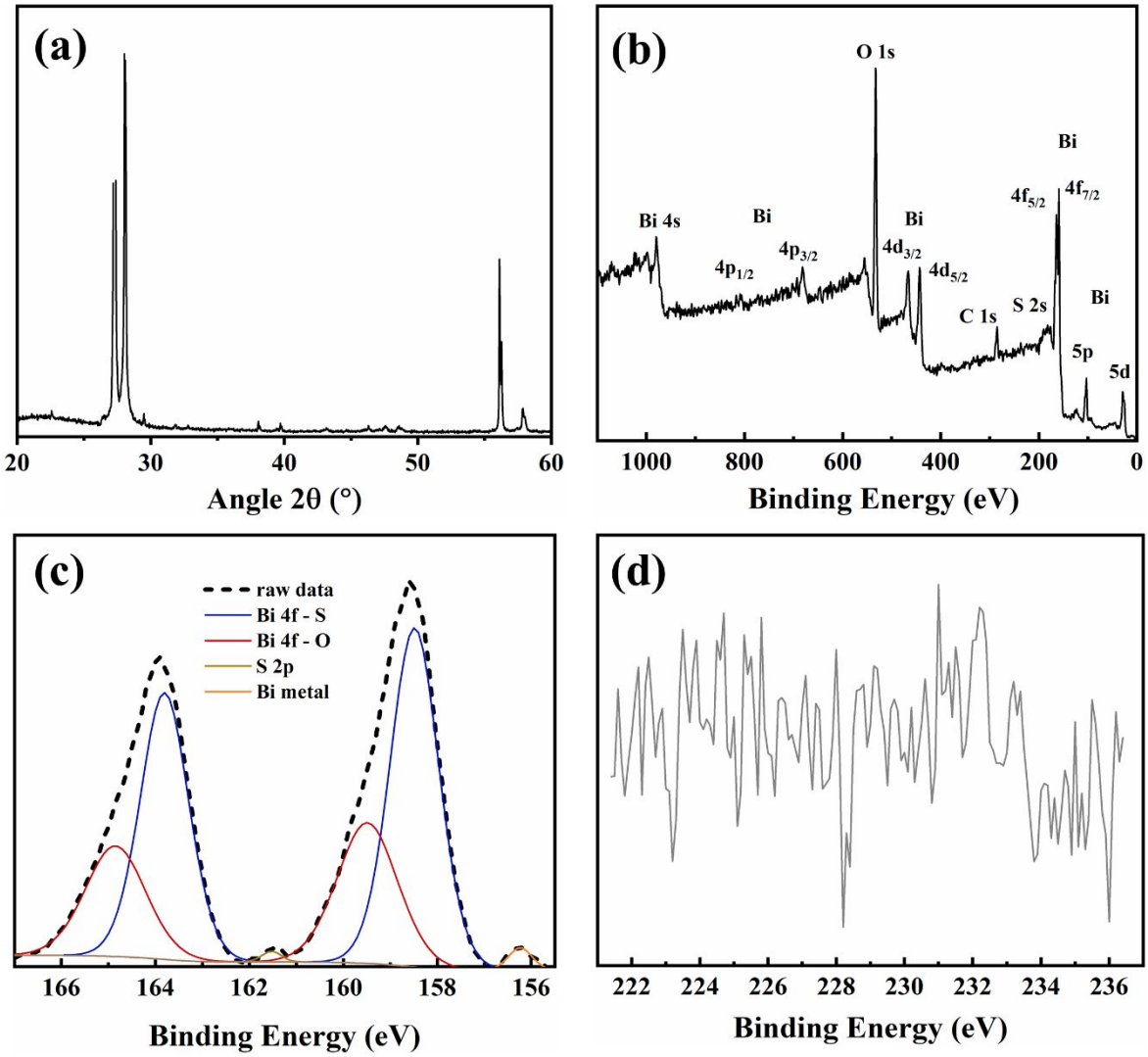

Figure S7. Characterisation of a pristine Bi_2S_3 film annealed at 400 °C: (a) x-ray diffraction pattern. The pattern does not match any file corresponding to Bi_2S_3, (b) XPS survey spectrum, (c) XPS core level for Bi 4f and (d) S 2s core level. The presence of a peak corresponding to metallic Bi indicates that almost all the sulfur has been removed, confirmed by the absence of peaks in the S 2s core level.

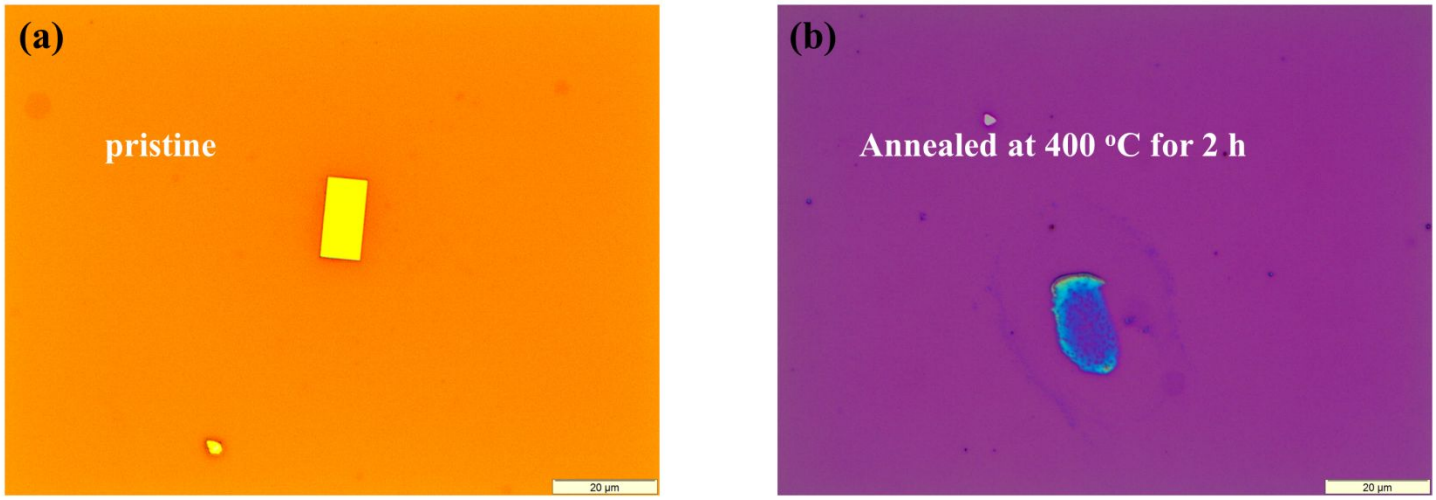

Figure S8. Optical images of a pristine Bi_2S_3 thin film: (a) as-patterned and (b) after annealing at 400 °C for 2 hours in a tubular furnace at a pressure below 10^{-2} Torr under forming gas (4% H_2, 96% N_2). After annealing the film suffers from delamination problems, despite Bi_2S_3 having a larger melting point. This indicated that the upper limit for S vacancy introduction in the directly written films is 400 °C, since the mechanical stability of the sample is compromised at this temperature.

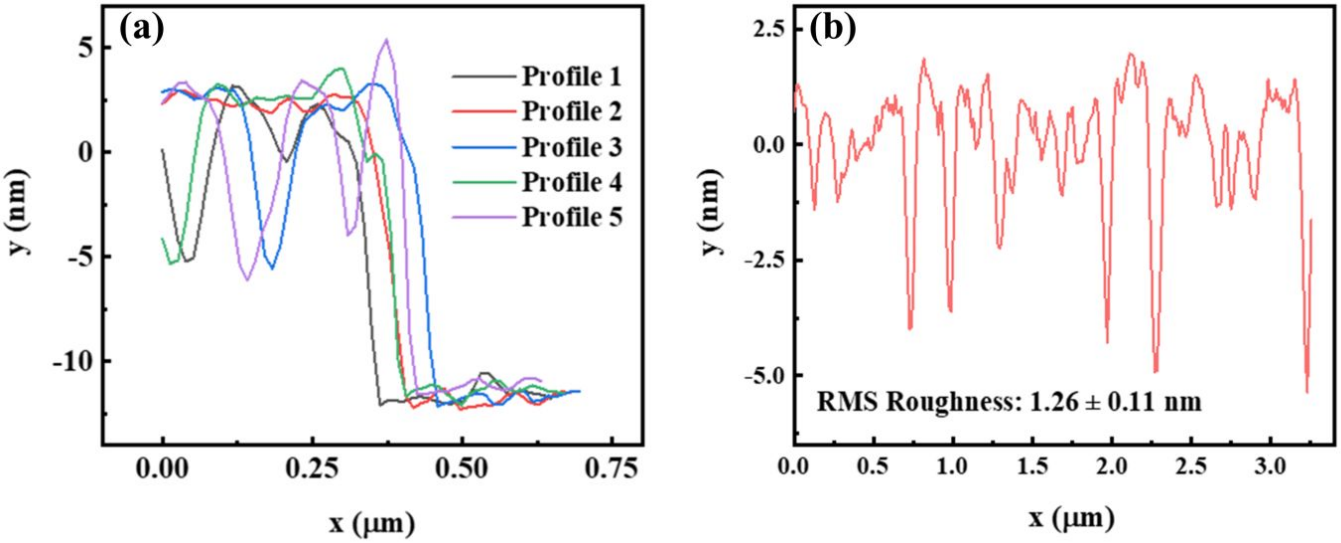

Figure S9. Extended AFM data for the directly written thin film annealed at 350 °C: (a) AFM height profiles and (b) RMS roughness measurement.

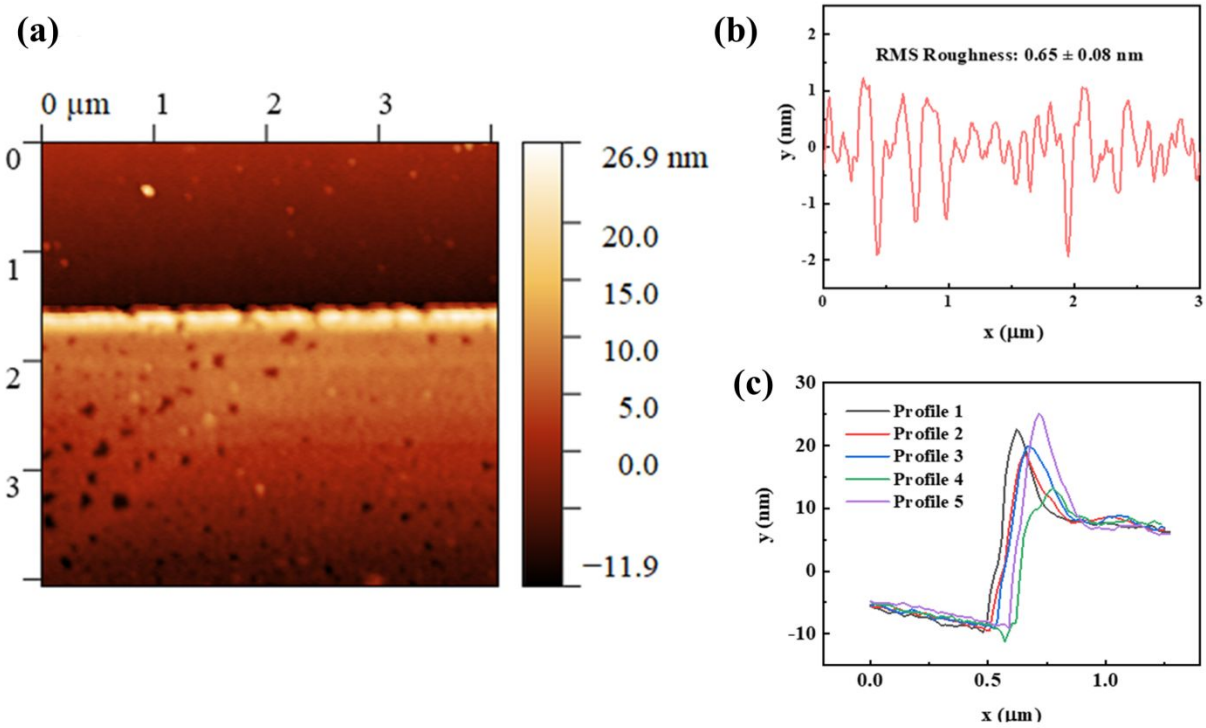

Figure S10. Extended AFM data for the directly patterned pristine thin film: (a) AFM tapping mode image, (b) RMS Roughness measurement and (c) AFM height profiles

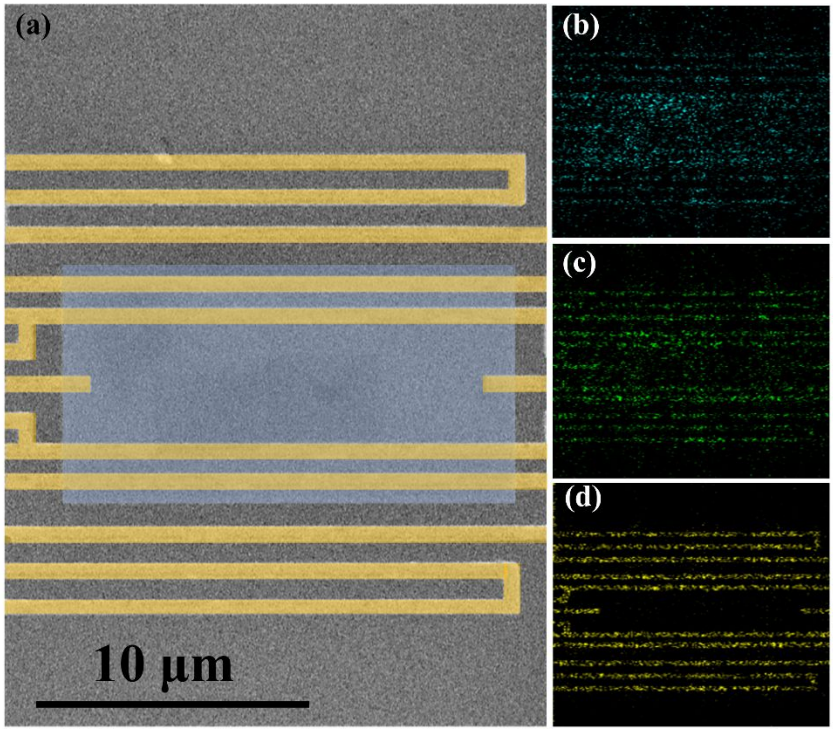

Figure S11. (a) SEM image used for EDX mapping, EDX map of (b) bismuth, (c) sulfur and (d) gold. The elemental composition of this film was determined to be 42.19 at. % of Bi and 57.80 at. % of sulfur.

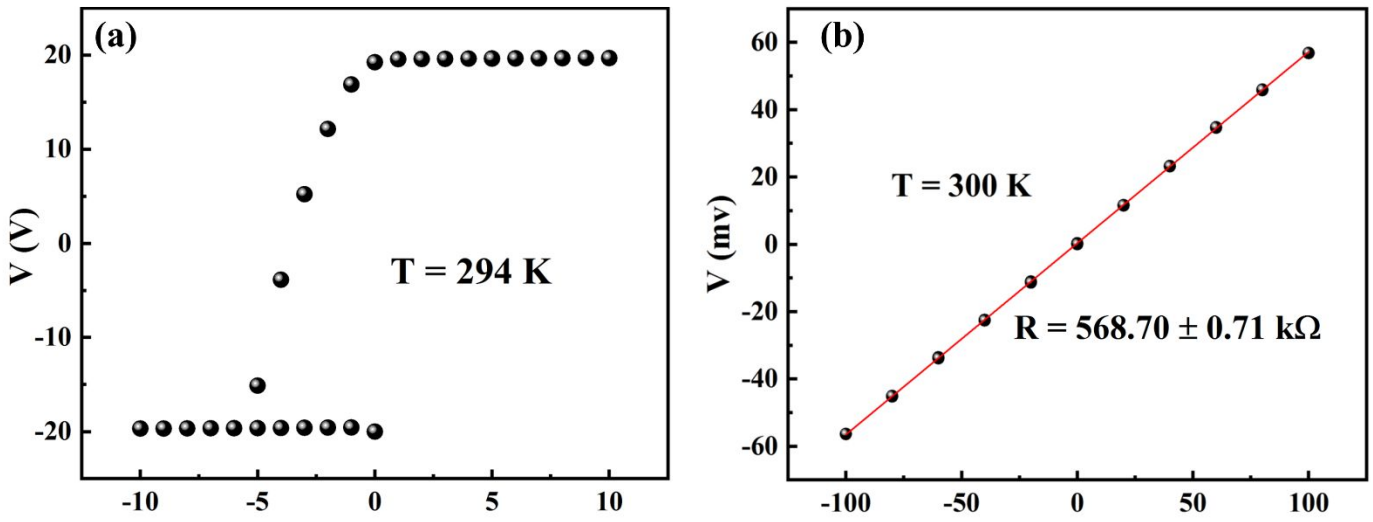

Figure S12. Room temperature four-point probe I-V curve for (a) directly written pristine Bi_2S_3 thin film showing an open circuit with no measurable resistance and (b) for a sub-stoichiometric Bi_2S_3 thin film, annealed for 2 hours at 350 °C in vacuum.

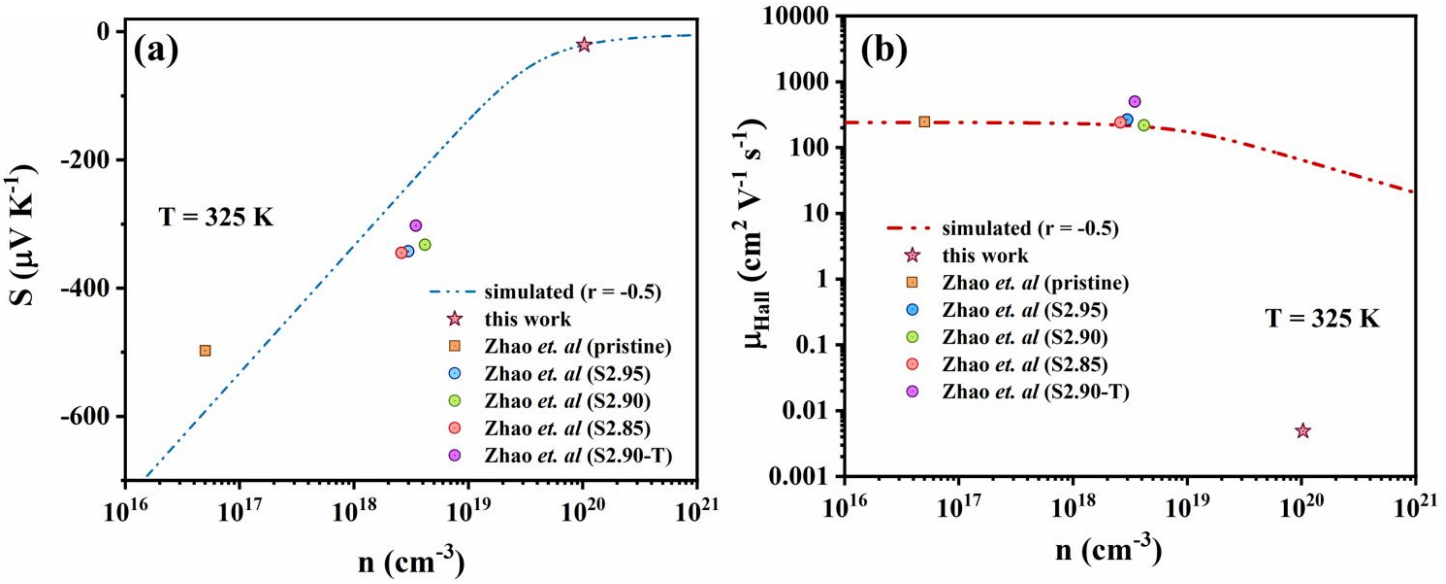

Figure S13. Near room temperature (a) Pisarenko relation (Seebeck coefficient *vs.* carrier concentration) and (b) mobility *vs.* carrier concentration for a sub-stoichiometric film (annealed under vacuum at 350 °C for 2 hours) and literature benchmark.[6] Simulated curves were obtained by solving the linearized Boltzmann Transport Equation[7], assuming acoustic phonon scattering (r = -0.5) and density-of-states effective mass, $m_{DOS} = 0.333m_e$.[8]

Supporting References

(1) Smith, G. C. *Surface Analysis by Electron Spectroscopy*; Springer US: Boston, MA, 1994. https://doi.org/10.1007/978-1-4899-0967-1.

(2) Huo, N.; Figueroba, A.; Yang, Y.; Christodoulou, S.; Stavrinadis, A.; Magén, C.; Konstantatos, G. Engineering Vacancies in Bi 2 S 3 Yielding Sub-Bandgap Photoresponse and Highly Sensitive Short-Wave Infrared Photodetectors. *Adv. Opt. Mater.* **2019**, *7* (11), 1900258. https://doi.org/10.1002/adom.201900258.

(3) Morgan, W. E.; Stec, W. J.; Van Wazer, J. R. Inner-Orbital Binding-Energy Shifts of Antimony and Bismuth Compounds. *Inorg. Chem.* **1973**, *12* (4), 953–955. https://doi.org/10.1021/ic50122a054.

(4) Grigas, J.; Talik, E.; Lazauskas, V. X-Ray Photoelectron Spectra and Electronic Structure of Bi2S3 Crystals. *Phys. status solidi* **2002**, *232* (2), 220–230. https://doi.org/10.1002/1521-3951(200208)232:2<220::AID-PSSB220>3.0.CO;2-F.

(5) Grigas, J.; Talik, E.; Lazauskas, V. X-Ray Photoelectron Spectra and Electronic Structure of Bi 2 S 3 Crystals. **2002**, *230* (2), 220–230.

(6) Zhao, L.-D.; Zhang, B.-P.; Liu, W.-S.; Zhang, H.-L.; Li, J.-F. Enhanced Thermoelectric Properties of Bismuth Sulfide Polycrystals Prepared by Mechanical Alloying and Spark Plasma Sintering. *J. Solid State Chem.* **2008**, *181* (12), 3278–3282. https://doi.org/10.1016/j.jssc.2008.08.022.

(7) Lundstrom, M. *Fundamentals of Carrier Transport*; Cambridge University Press: Cambridge, 2000. https://doi.org/10.1017/CBO9780511618611.

(8) Gorai, P.; Gao, D.; Ortiz, B.; Miller, S.; Barnett, S. A.; Mason, T.; Lv, Q.; Stevanović, V.; Toberer, E. S. TE Design Lab: A Virtual Laboratory for Thermoelectric Material

Design. *Comput. Mater. Sci.* **2016**, *112*, 368–376.

https://doi.org/10.1016/j.commatsci.2015.11.006.